Journal of Solid State Chemistry 181 (2008) 1650–1658

Contents lists available at ScienceDirect

Journal of Solid State Chemistry

journal homepage: www.elsevier.com/locate/jssc

Jingle-bell-shaped ferrite hollow sphere with a noble metal core: Simple synthesis and their magnetic and antibacterial properties

Siheng Li, Enbo Wang *, Chungui Tian, Baodong Mao, Zhenhui Kang, Qiuyu Li, Guoying Sun

Key Laboratory of Polyoxometalate Science of Ministry of Education, Department of Chemistry, Northeast Normal University, Changchun, Jilin 130024, People's Republic of China

ARTICLE INFO

Article history:
Received 11 March 2008
Received in revised form
2 May 2008
Accepted 16 May 2008
Available online 21 May 2008

Keywords:
Hollow spheres
Ferrite
Metal nanoparticles
Magnetic properties
Antibacterial properties

ABSTRACT

In this paper, a simple strategy is developed for rational fabrication of a class of jingle-bell-shaped hollow structured nanomaterials marked as Ag@MFe$_2$O$_4$ (M = Ni, Co, Mg, Zn), consisting of ferrite hollow shells and metal nanoparticle cores, using highly uniform colloidal Ag@C microspheres as template. The final composites were obtained by direct adsorption of metal cations Fe^{3+} and M^{2+} on the surface of the Ag@C spheres followed by calcination process to remove the middle carbon shell and transform the metal ions into pure phase ferrites. The as-prepared composites were characterized by X-ray photoelectron spectroscopy (XPS), energy-dispersive X-ray analysis (EDX), X-ray powder diffraction (XRD), scanning electron microscopy (SEM), transmission electron microscopy (TEM), UV–vis spectroscopy and SQUID magnetometer. The results showed that the composites possess the magnetic property of the ferrite shell and the optical together with antibacterial property of the Ag core.

1. Introduction

Recently, lots of interest has been focused on the fabrication of advanced materials with core–shell structure owing to their unique optical, electronic and catalytic properties and versatile applications because that the core–shell composites might exhibit dual properties of the core and shell materials [1–4]. Noble metal nanoparticles (NPs) are of great interest due to their excellent optical, electric and catalytic properties and potential applications in many areas [5–8]. The combination of noble metal NPs with other materials to form a core–shell composite have been a research hotspot because of the broad tune of core and shell materials, and consequently, the properties of the resulting composites. Many kinds of the composites have been successfully fabricated, such as metal particles modified with organic polymer or inorganic oxides shell and core colloids decorated with metal NPs [9–13]. In recent years, a class of new core–shell materials consisting of metal NP cores in hollow shell, namely jingle-bell-shaped composite colloids, have been prepared and attracted much new interest because of the internal freedom of the core particle [14–16]. For instance, Xia and co-workers synthesized hollow colloidal spheres with movable Au NP cores by dissolving the middle silica shell between the Au core and the polymer shell [17]. Jingle-bell-shaped pure cobalt hollow spheres, with which magnetic chains of jingle-bell-shaped cobalt hollow spheres have been generated, were fabricated by the one-step solution route [18]. Nanosized Sn metal particles encapsulated in hollow carbon spheres have been prepared by heat treatment followed by cooling, which results in different extents of volume change for Sn and C [15]. The obvious similarity in the above-mentioned researches is the multi-step preparation processes including pre-formation of metal NPs, encapsulation of metal cores in the middle shell, surface modification for templates and achievement of final products. Thus, exploring simple procedures for obtaining those materials is still a fascinating research hotspot.

Recently Y.D. Li's group reported the synthesis of monodisperse metal@C core–shell microspheres (Ag@C and Au@C) by a simple one-step process [19,20]. The exterior of the Ag@C core–shell nanospheres is hydrophilic and possesses abundant −OH and −C═O groups similar to the pure colloid carbon sphere [19–22], which makes surface modification unnecessary when they are used as template. Here we developed a facile method for the fabrication of jingle-bell-shaped Ag@MFe$_2$O$_4$ (M = Ni, Co, Mg, Zn) hollow sphere based on the colloidal Ag@C core–shell microspheres as templates. Two obvious advantages may be observed in the methods. First, the formation of metal NPs and the encapsulation into carbon shell were performed in a "one-step" fashion, avoiding complicated multi-step reaction process including formation of metal NPs and subsequent modification of the interior shell. Secondly, the abundant –OH and –C═O groups make the Ag@C core–shell colloids easy interact with various metal ions with no need of surface modification. Experimental results demonstrated that the jingle-bell-shaped Ag@MFe$_2$O$_4$

* Corresponding author. Fax: +86 431 509 8787.
E-mail addresses: Wangeb889@nenu.edu.cn, wangenbo@public.cc.jl.cn (E. Wang).

0022-4596/$ - see front matter © 2008 Elsevier Inc. All rights reserved.
doi:10.1016/j.jssc.2008.05.021

(M = Ni, Co, Mg, Zn) hollow spheres could be easily prepared by using colloidal Ag@C core–shell microspheres as sacrificial templates. The composites were obtained by direct adsorption of Fe^{3+} and M^{2+} on the surface of Ag@C microspheres followed by a simple calcination process, which were used to remove the middle carbon shell and to transform the metal ions into pure phase ferrites. Experimental results showed that the composites possessed the optical property and the outstanding antibacterial property of the Ag NPs and the magnetic property of the ferrite shells. Also, the primary results demonstrated that this method could be expanded to prepare a class of ferrite hollow shells with various metal NP cores.

2. Experimental

2.1. Materials

All chemicals, $AgNO_3$, $HAuCl_4$, NaCl, glucose, $Fe(NO_3)_3 \cdot 9H_2O$, $Ni(NO_3)_2 \cdot 6H_2O$, $Co(NO_3)_2 \cdot 6H_2O$, $Mg(NO_3)_2 \cdot 2H_2O$ and $Zn(Ac)_2 \cdot 2H_2O$ are of analytical grade and used as received without further purification. *Escherichia coli* (*E. coli*) DH5α cells, tryptone, yeast extract and agar were purchased from Takara Biotechnology Co., Ltd. (Dalian, P.R. China).

2.2. Synthesis

2.2.1. Preparation of Ag@C core–shell colloids

The colloidal Ag@C composite colloids were prepared according to the reported method developed by Sun and Li [20]. In a typical synthesis of Ag@C colloids with diameter of about 400 nm, 4 g of glucose was dissolved in 35 mL of water to form a clear solution. After that 0.5 mL of 0.1 M $AgNO_3$ aqueous solution was added dropwise into the glucose solution under vigorous stirring for about 30 min. Then the solution was transferred and sealed in a 40 mL Teflon-sealed autoclave. After hydrothermal reaction at 160 °C for 12 h, the autoclave was cooled to room temperature naturally in air. The suspensions of the products were deep brown in color. The final products were separated from the reaction medium by centrifuging at 5000 rpm for 30 min. A rinsing process including three cycles of centrifugation/washing/redispersion procedures with deionized water and ethanol was required before oven drying at 80 °C for 10 h.

2.2.2. Preparation of jingle-bell-shaped Ag@MFe_2O_4 (M = Ni, Co, Mg, Zn) hollow sphere

All the ferrite hollow spheres were prepared following the same procedure. For example, for a typical synthesis procedure of Ag@$NiFe_2O_4$ hollow spheres, 50 mg Ag@C colloids were ultrasonically dispersed in 5 mL aqueous solution of $Fe(NO_3)_3 \cdot 9H_2O$ and $Ni(NO_3)_2 \cdot 6H_2O$ (total concentration of metal cations was 1 M with the Fe^{3+}:M^{2+} molar ratio was 2:1). The resulting colloidal solution was aged for 12 h before centrifugation and washed with distilled water and ethanol for three times. The as-prepared composites were dried at 100 °C for 1 h and calcined at 550 °C in air for 5 h in a muffle furnace to remove the intermediate carbon shell. After cooling to room temperature naturally in air, the jingle-bell-shaped Ag@$NiFe_2O_4$ hollow spheres were obtained. For the synthesis of Ag@$CoFe_2O_4$, Ag@$MgFe_2O_4$ and Ag@$ZnFe_2O_4$, $Co(NO_3)_2 \cdot 6H_2O$, $Mg(NO_3)_2 \cdot 2H_2O$ and $Zn(Ac)_2 \cdot 2H_2O$ are used instead of $Ni(NO_3)_2 \cdot 6H_2O$ in the above-mentioned procedure, respectively.

2.3. Characterization

Transmission electron microscopy (TEM, Hitachi-7500, operating voltage of 120 kV) and scanning electron microscopy (SEM, JEOL JSM-840 operated at 20 kV) were used to characterize the particle size and morphology. X-ray powder diffraction (XRD) patterns were measured using a Rigaku D/max-IIB X-ray diffractometer at a scanning rate of 4° per minute with 2θ ranging from 10° to 90°, using Cu $K\alpha$ radiation ($\lambda = 1.5418$ Å). Magnetic measurements were carried out on a Quantum Design MPMS-XL5 SQUID magnetometer at room temperature with the field sweeping from −10,000 to 10,000 Oe. X-ray photoelectron spectroscopy (XPS) analysis combined with energy-dispersive X-ray analysis (EDX) has been done in order to obtain information about the chemical composition of templates and final products. UV–visible spectra were recorded with a 756 CRT UV–vis spectrophotometer. IR spectra were recorded in the range 400–4000 cm^{-1} on an Alpha Centauri FT/IR spectrophotometer by use of KBr pellets.

3. Results and discussion

A simplified schematic synthesis process is shown in Scheme 1. First, the Ag@C core–shell microspheres were obtained by a simple one-step process. As reported previously, the surface of the colloidal Ag@C microspheres is hydrophilic and has an ample distribution of OH and C=O groups, which could be used to reduce noble metals or to absorb metal ions [23–25]. After Ag@C core–shell spheres were ultrasonically dispersed in solutions of metal salts solution, two kinds of metal cations (Fe^{3+} and M^{2+}) were adsorbed onto the carbon shell, which is called "metals as-adsorption" process here. Then, the ferrite hollow spheres were

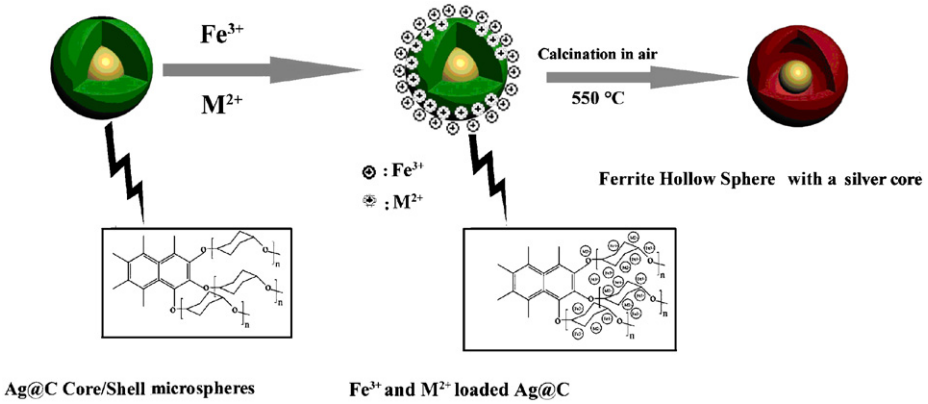

Scheme 1. Schematic process for synthesis of the ferrite hollow spheres with a metal nanoparticle core.

obtained by a simple calcination of the above precursor spheres to remove the carbon intermediate shell and to transform the metal components to pure phase ferrites.

3.1. Characterizations of colloidal Ag@C core–shell spheres

The formation of Ag@C core–shell spheres were demonstrated by TEM, SEM, EDX and XRD. The TEM image (Fig. 1a) and SEM images (Fig. 1b and c) indicated that the Ag@C colloids were highly uniform with the size in a narrow range 360–380 nm. Fig. 1b and c are the SEM images of the Ag@C core–shell spheres with different magnification, indicating that the samples were highly uniform. From Fig. 1a, Ag NPs cores with the size of 60–70 nm in samples can be clearly observed. The EDX in Fig. 1e confirmed the presence of Ag, C and O in the Ag@C nanospheres (Pt peaks were due to the platinum coating on glass slide when investigating SEM).

In the XRD patterns of Ag@C microspheres shown in Fig. 1d, five diffraction peaks corresponding to the (111), (200), (220), (311) and (222) reflections of face-centred cubic (fcc) structured metal Ag (PDF: 4-783) are observed at $2\theta = 38.2^\circ$, 44.3°, 64.4°, 77.5° and 81.4°, indicating the presence of Ag phase in the sample. UV–vis spectrum of the Ag@C core–shell colloids (Fig. 2, Curve a) shows an adsorption peak at about 430 nm and no other peaks are found in the range 400–800 nm, also indicating the existence of Ag NPs [26–29].

FTIR spectrum was used to identify the functional groups on the surface of Ag@C nanospheres as shown in Fig. 3. The absorption bands at $\upsilon = 1710$ and $1620\,cm^{-1}$ are attributed to C═O and C═C vibrations, and the bands in the range $\upsilon = 1000$–$1300\,cm^{-1}$ are attributed to the C–OH stretching and OH bending vibrations, supporting the existence of large amount of residual hydroxyl groups, which could be covalently bonded to metal ions without any surface modification when uniform Ag@C microspheres used as template. The above results are in accord with previous study of the core–shell carbonaceous spheres [19]. Thus, without any additional surface modification of Ag@C microspheres, the jingle-bell-shaped Ag@MFe$_2$O$_4$ hollow spheres were prepared by first adsorption of Fe^{3+} and M^{2+} on the surface of Ag@C microspheres followed by a simple calcination process in air.

3.2. The morphology analysis of Ag@MgFe$_2$O$_4$ hollow spheres

Fig. 4a shows the TEM image of the Ag@MgFe$_2$O$_4$ hollow spheres. It can be seen that the hollow spheres (160–180 nm) with shell thickness of about 25 nm (Fig. 4a) are much smaller than the

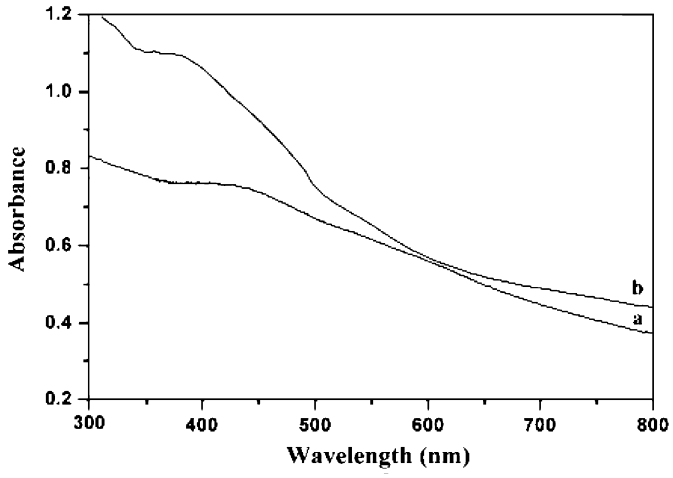

Fig. 2. UV–vis absorption spectra of the Ag@C microspheres (a) and (b) Ag@MgFe$_2$O$_4$ hollow spheres prepared when total concentration of metal cations (Fe^{3+} and M^{2+}) was 1 M.

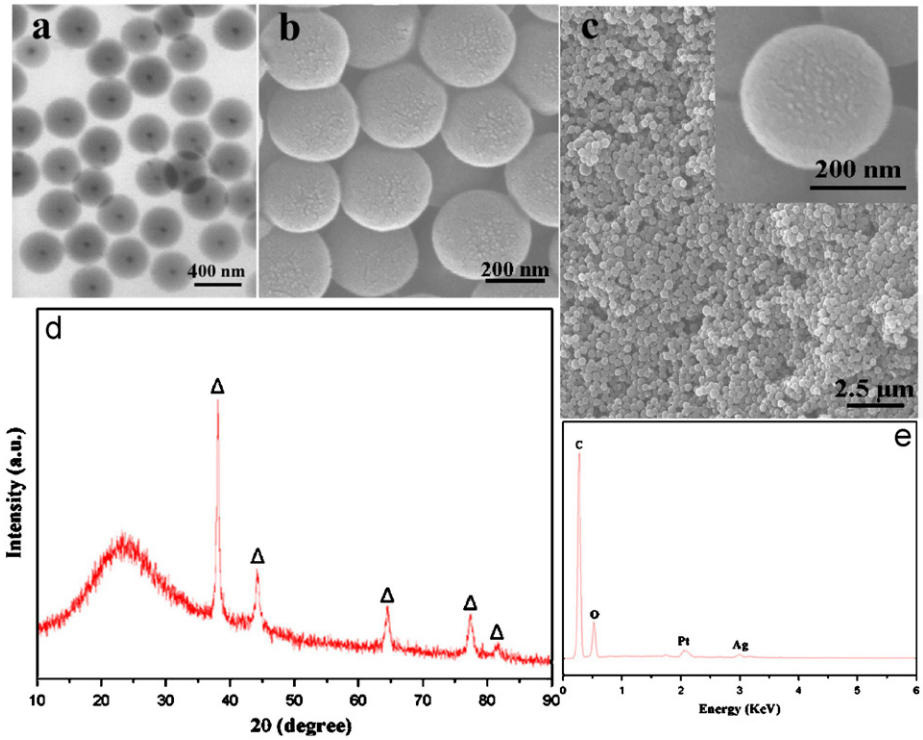

Fig. 1. Typical TEM image (a), SEM images (b and c), XRD pattern (d) and EDX spectrum (e) of the colloidal Ag@C core–shell microspheres.

templates. The size of Ag NPs cores in the jingle-bell-shaped structures was in range of 20–30 nm as shown in Fig. 4a. The decrease of the size of Ag cores after calcination may probably be due to that the Ag NPs melted and evaporated partially during the calcination process. Moreover, the ferrite hollow spheres underwent obvious shrinkage after the calcination process, which is probably caused by further dehydration of the loosely cross-linked structure of the carbon shell of the templates [21].

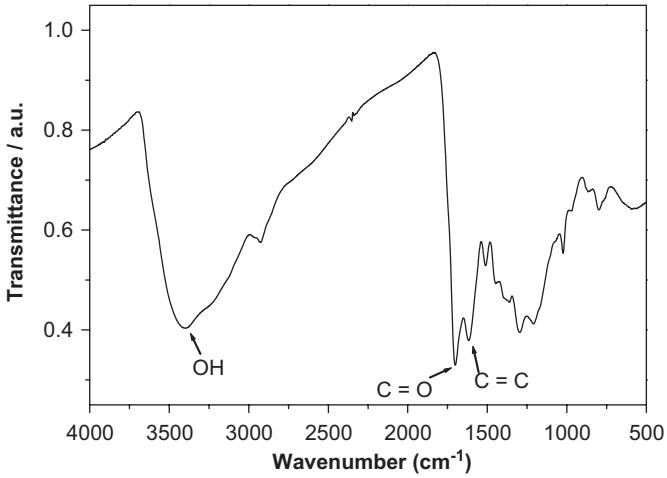

Fig. 3. FTIR spectrum of the Ag@C core–shell colloids.

The SEM image shown in Fig. 4b was used to observe the size and morphology of the Ag@$MgFe_2O_4$ hollow spheres when total concentration of metal cations (Fe^{3+} and M^{2+}) was 1 M. It can be seen that the size of $MgFe_2O_4$ hollow spheres was in the range of 160–180 nm (same results as TEM) with narrow size distribution and the shells of the $MgFe_2O_4$ hollow spheres were consisted of closely packed NPs. Shell thickness of the hollow spheres is of about 25 nm. In comparison with Fig. 1, the size of ferrite hollow spheres is further smaller than the as-prepared Ag@C spheres as shown in Fig. 3, which were consistent with the results obtained in the TEM observation. It should be pointed out that various sizes of ferrite hollow spheres with silver core can also be obtained because the size of Ag@C nanospheres could be well tuned via adjusting the various reaction conditions, such as reaction time and temperature as described in previous reports [20]. The elemental composition demonstrated by EDX shown in Fig. 4c proved the presence of Ag, Mg, Fe and O in the final samples, further confirmed the formation of the ferrites with silver cores.

3.3. XRD and XPS analysis of Ag@$MgFe_2O_4$ hollow spheres

Fig. 5 gives the XRD pattern of the Ag@$MgFe_2O_4$ hollow spheres prepared with 1 M metal cations (Fe^{3+} and M^{2+}). Five

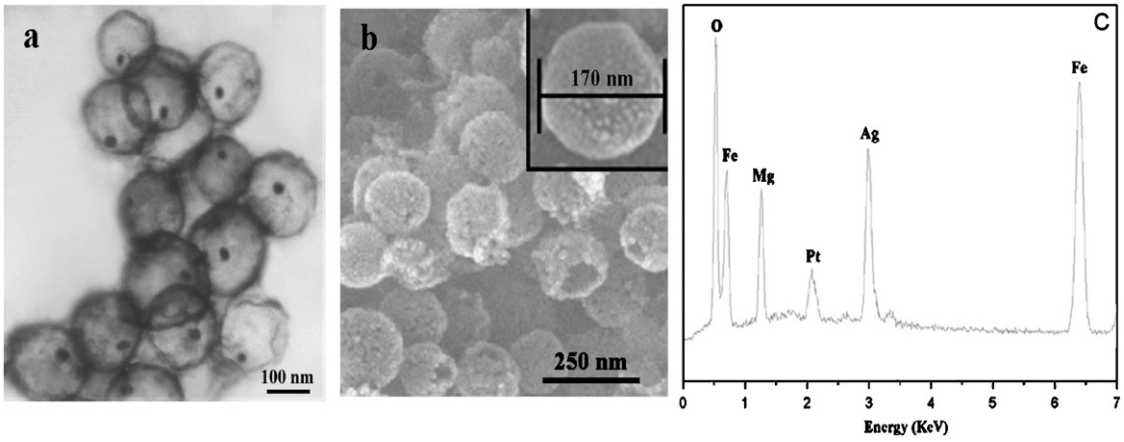

Fig. 4. Typical (a) TEM, (b) SEM images and (c) EDX spectrum of Ag@$MgFe_2O_4$ hollow spheres prepared when total concentration of metal cations (Fe^{3+} and M^{2+}) was 1 M.

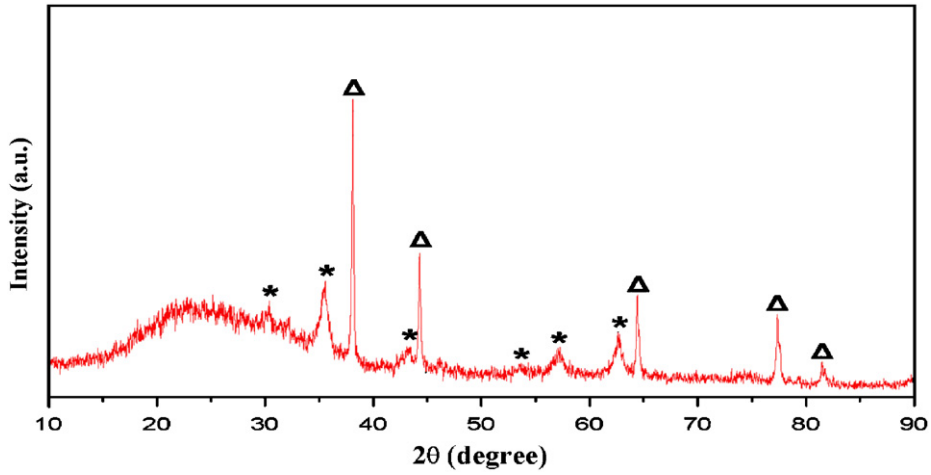

Fig. 5. XRD pattern of the Ag@$MgFe_2O_4$ hollow spheres prepared with total concentration of metal cations (Fe^{3+} and M^{2+}) was 1 M.

diffraction peaks are observed almost the same at $2\theta = 38.2^\circ$, 44.3°, 64.4°, 77.5° and 81.4° corresponding to the (111), (200), (220), (311) and (222) reflections of fcc structured metal Ag (PDF: 4-783), indicating the presence of Ag NPs. In addition, the UV–vis result of the composites with an adsorption peak at about 390 nm (Fig. 2, Curve b), also confirming the existence of Ag NPs in final products [26–29]. Besides the Ag phases, the other peaks can be easily indexed as fcc phase ferrite $MgFe_2O_4$ (JCPDS PDF 88-1943).

XPS is an effective tool for analyzing elements and their corresponding valence state. The Ag@$MgFe_2O_4$ hollow spheres were characterized by XPS. The peak at 529.8 eV in Fig. 6a is attributed to O 1*s*. The Ag $3d_{5/2}$ peak is locating at about 368.1 eV (Fig. 6b), indicating the presence of Ag^0 in the samples. The observation of Fe 2*p* at 711.5 ($2p_{3/2}$) and 724.9 ($2p_{1/2}$) (Fig. 6c) and the Mg 2*p* core level at 49.58 eV BE (Fig. 6d) proves the formation of magnesium ferrite [30–33]. In summary, the XPS studies further demonstrated the formation of the Ag@$MgFe_2O_4$ spheres in our experiments.

3.4. Magnetic property of Ag@$MgFe_2O_4$ hollow spheres

In order to study magnetic property of the ferrite hollow spheres with Ag cores, the magnetic study was performed with a Quantum Design MPMS-XL5 SQUID magnetometer at 300 K (room temperature) and 2 K by cycling the field between −10,000 and 10,000 Oe (Fig. 7). The samples of the Ag@$MgFe_2O_4$ hollow spheres were prepared with 1 M total concentration of metal

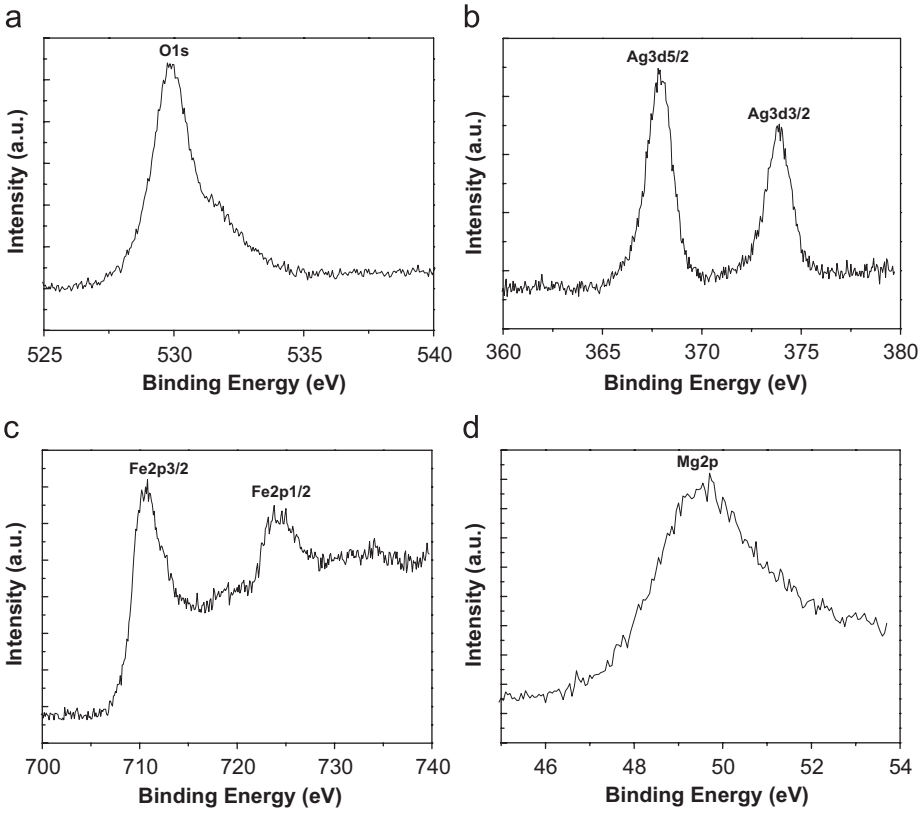

Fig. 6. XPS spectra of O 1*s*, Ag 3*d*, Fe 2*p* and Mg 2*p* of the Ag@$MgFe_2O_4$ hollow spheres.

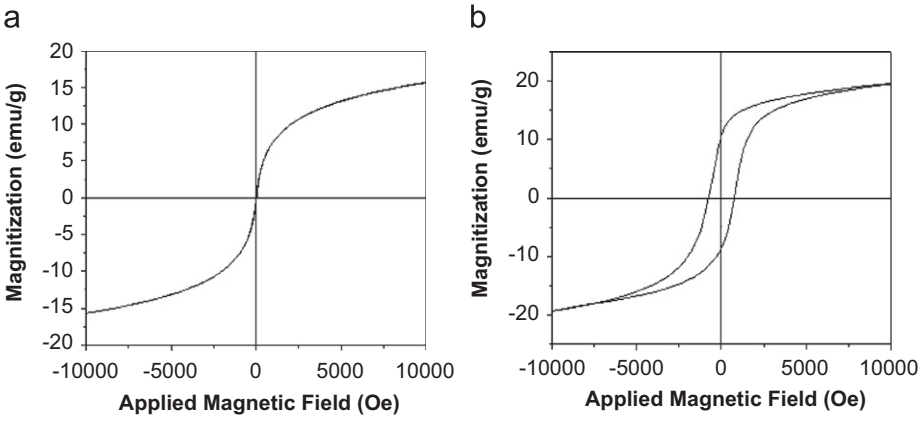

Fig. 7. Magnetization hysteresis loops of Ag@$MgFe_2O_4$ hollow spheres prepared when total concentration of metal cations (Fe^{3+} and M^{2+}) was 1 M, measured at (a) 300 K and (b) 2 K.

cations. It could be seen that there is no hysteresis, and both remanence and coercivity are zero (Fig. 7a), suggesting that the magnesium ferrite shells are superparamagnetic at room temperature with the saturation magnetization was 15.7 emu/g. As shown in Fig. 7b, the Ag@$MgFe_2O_4$ samples possessed a ferromagnetic behavior at 2 K. The saturation magnetization (M_s), remanent magnetization (M_r), and coercivity (H_c) values are ca. 19.44 emu/g, 10.65 emu/g and 764.8 Oe, respectively.

Superparamagnetism [34,35], responsiveness to an applied magnetic field without permanent magnetization, is an especially important property needed for magnetic separation because it ensures repeated use of magnetic materials or combined functional materials (such as noble metal NPs) and efficient product elution. The magnetic separability of such magnetic composites was tested in ethanol by placing a magnet near the glass bottle. As shown in Fig. 8, the particles were attracted toward the magnet within 10 s, demonstrating directly that the jingle-bell-shaped composites could be easily separated from water by applying a magnetic field. This will provide an easy and efficient way to separate the composites from a sol or a suspension system and to lead functional metal NPs to targeted locations in reaction systems with an external magnetic field.

3.5. Antibacterial properties of Ag@$MgFe_2O_4$ hollow spheres

There is an increasing interest in utilization of nano-Ag as a special class of biocidal agents owing to the extraordinary antimicrobial properties [36–40]. There are also a number of silver composite materials that contain nano-Ag as the active antimicrobial ingredient. The antibacterial activities of the ferrite hollow spheres with a silver core (Ag@$MgFe_2O_4$ was chosen as a model) was tested on *E. coli* by the standard disk diffusion assay on LB agar medium, as the bacteria were very common and they caused a typical infection to human body. All glassware and materials were sterilized in autoclave at 120 °C for 20 min before experiments. The disk diffusion assay was performed by placing an 8 mm filter paper treated with 20 μL of Ag@$MgFe_2O_4$ nanocomposite aqueous slurry (10 mg/L) onto an agar plate seeded with approximate 10^7 colony forming units (CFU) of *E. coli* (Fig. 9a). Then the plate was incubated at 37 °C for 24 h. Results were recorded by measuring the diameter of inhibition zones for four times (Table 1). Additionally, the control cultures (in absence of samples) used as negative comparison were maintained to check for growth of the *E. coli* (Fig. 9b). The minimum bactericidal concentration (MBC) of commonly used antibiotics viz. streptomycin was also applied to compare the

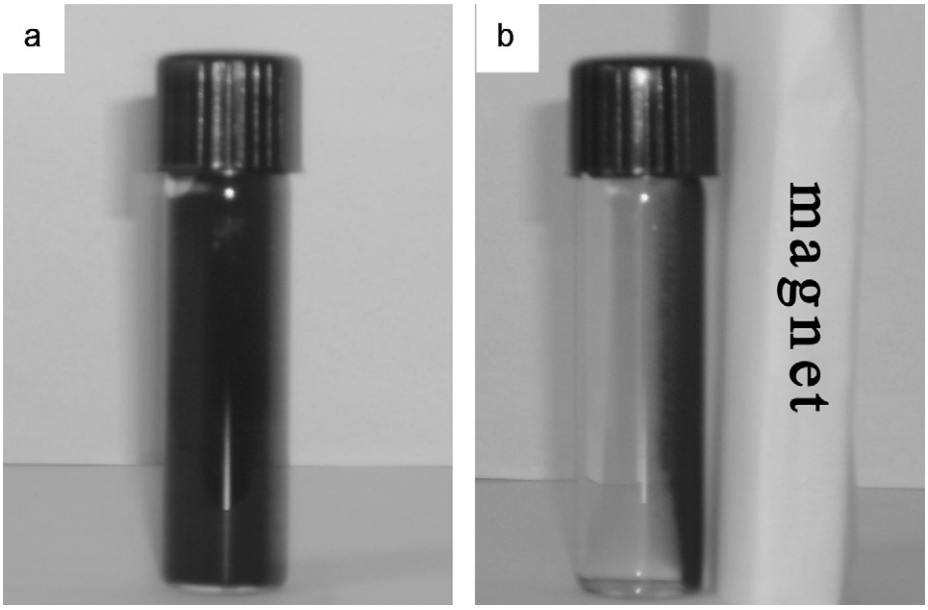

Fig. 8. Photograph of separation of Ag@$MgFe_2O_4$ hollow spheres from solution under an external magnetic field.

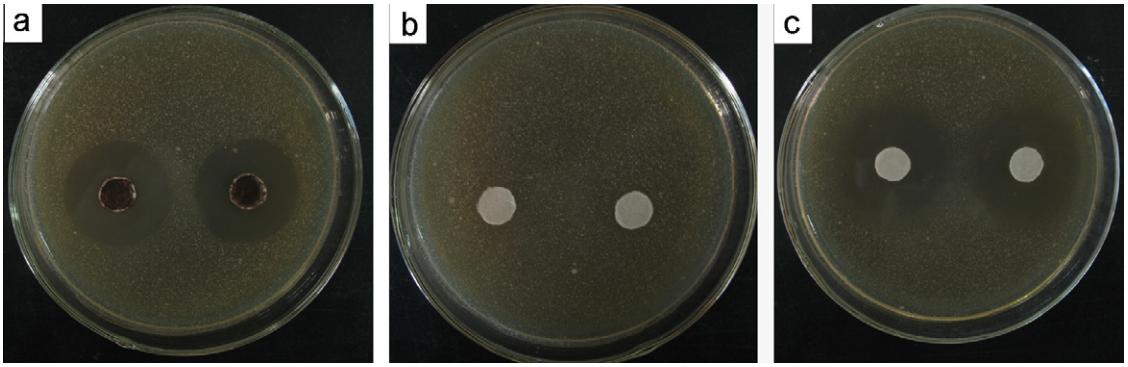

Fig. 9. Photographs of the antibacterial test on *E. coli* after 24 h: (a) incubated with Ag@$MgFe_2O_4$, (b) the control and (c) incubated with streptomycin.

antibacterial effectiveness of the $Ag@MgFe_2O_4$ nanocomposite (Fig. 9c). The above results revealed the good antibacterial activities of the resulted composites.

3.6. Characterizations of other jingle-bell-shaped ferrite hollow spheres with Ag cores and the effect of preparation conditions on the products

Besides $Ag@MgFe_2O_4$, other ferrite hollow spheres were also prepared by the same method to confirm the generality of the present process. The XRD patterns of the as-prepared $Ag@ZnFe_2O_4$ and $Ag@CoFe_2O_4$ are shown in figure S2 when total concentration of metal cations (Fe^{3+} and M^{2+}) was 1 M. Five diffraction peaks were observed at $2\theta = 38.2^\circ$, 44.3°, 64.4°, 77.5° and 81.4° corresponding to the (111), (200), (220), (311) and (222) reflections of fcc structured metal Ag (PDF: 4-783), indicating the presence of Ag NPs. The UV–vis spectra of $Ag@ZnFe_2O_4$ (figure S3, Curve a) and $Ag@CoFe_2O_4$ (figure S3, Curve b) with an adsorption peak at about 380 nm also indicates the existence of Ag NPs core [26–29]. Moreover, the XRD patterns can also be easily indexed to fcc phase $ZnFe_2O_4$ (figure S2, pattern a, JCPDS 22-1012) and $CoFe_2O_4$ (figure S2, pattern b, JCPDS 22-1086). Thus the present method is demonstrated to be an effective way for preparing series of transition metal ferrite hollow spheres with an Ag core. As ferrites represent an important class of low cost and widely used technological magnetic materials, the as-prepared ferrite hollow spheres may meet the need of future applications.

Table 1
Antibacterial assay by disc diffusion method for $Ag@MgFe_2O_4$ nanocomposite

Samples	Diameter of inhibition zones (mm)				
	1	2	3	4	Average
$Ag@MgFe_2O_4$	29.2	29.4	29.2	29.3	29.3
Streptomycin	33.2	33.4	33.3	33.2	33.3

The influence of concentration of the metal cations on the final ferrite hollow spheres was also investigated. The XRD patterns of the nickel ferrite hollow structures prepared on various conditions were also obtained as shown in Fig. 10. For patterns a–c, the hollow spheres can be perfectly indexed as fcc nickel ferrite with lattice constant $a = 8.393$ Å (JCPDS no. 82-1533). From pattern a to pattern c (corresponding total concentration of metal cations was 1, 0.5 and 0.25 M, respectively), the diffraction peaks of $NiFe_2O_4$ hollow spheres show a continuous decrease with the decrease of the metal concentration, while peaks of Ag phase becomes stronger contrarily. It was probably due to that the relative content of ferrites shell decreased when total concentration of metal cations was reduced.

Additionally, the magnetic behavior of the composites obtained with two different concentrations of metal cations (1 and 0.25 M) was also studied. Fig. 11 shows the magnetization curves of $Ag@NiFe_2O_4$ composites at 300 and 2 K. Similar to the $Ag@MgFe_2O_4$, it is superparamagnetic at room temperature (Fig. 11a) with the saturation magnetization changed from 15.35 to 13.40 emu/g when total concentration of metal cations was adjusted from 1 to 0.25 M. The composite possessed a ferromagnetic behavior at 2 K with M_s, M_r and H_c changed from 34.22 emu/g, 18.69 emu/g, 883.92 Oe to 27.71 emu/g, 14.09 emu/g, 685.4 Oe when total concentration of metal cations was adjusted from 1 to 0.25 M (Fig. 11b). The saturation magnetization similarly decreases along with decrease of concentration of metal ions. The results confirm that the magnetic properties of the composites could be tuned by varying concentration of metal cations.

3.7. Characterizations of colloidal Au@C and Au@MFe_2O_4 spheres

It is well known that colloidal core–shell carbon spheres with various metal NP cores could also easily be obtained via

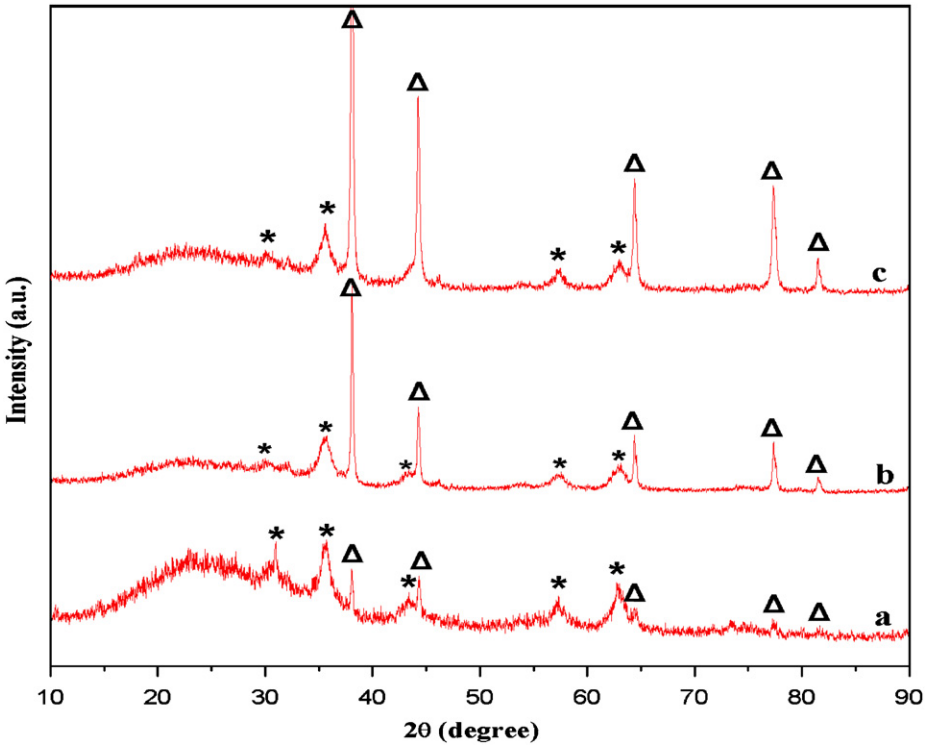

Fig. 10. XRD patterns of $Ag@NiFe_2O_4$ hollow structures prepared with different total concentration of metal cations (Fe^{3+} and M^{2+}): (a) 1 M, (b) 0.5 M, and (c) 0.25 M.

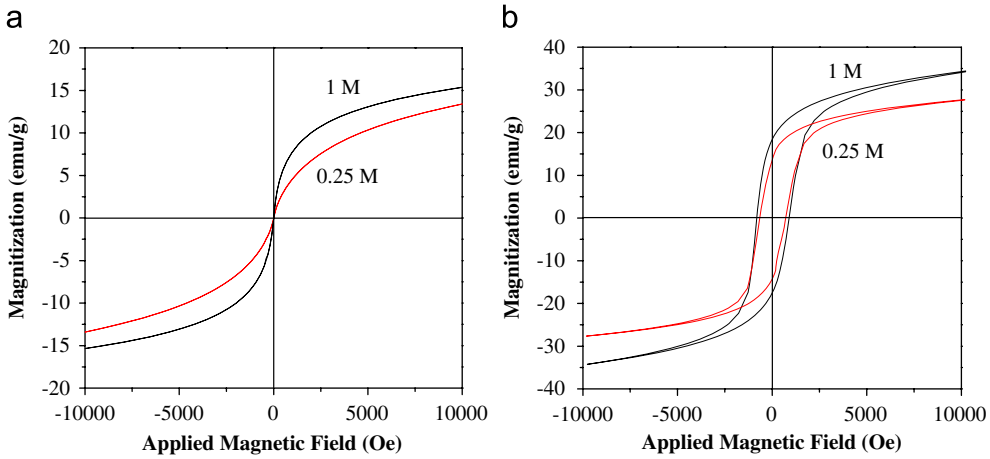

Fig. 11. Magnetization hysteresis loops of Ag@$NiFe_2O_4$ hollow spheres prepared with two different total concentrations of metal cations (Fe^{3+} and M^{2+}) measured at (a) 300 K and (b) 2 K.

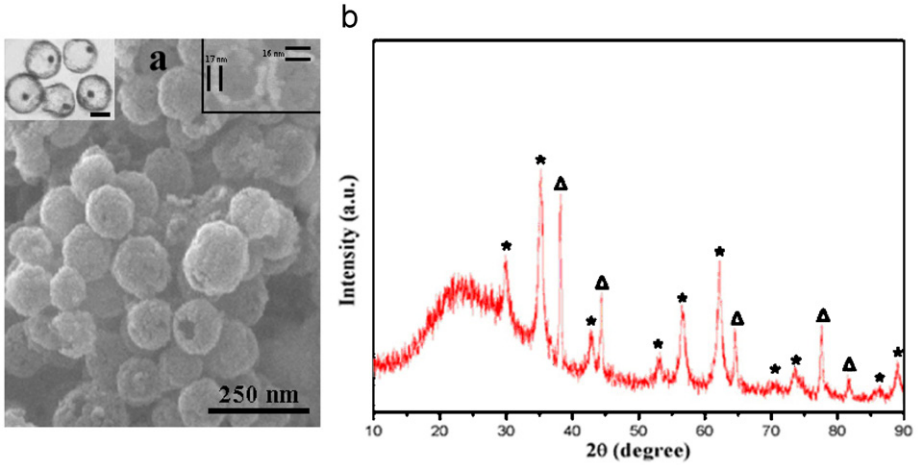

Fig. 12. Typical TEM and SEM images (a) and XRD pattern of Au@$MgFe_2O_4$ hollow sphere prepared when total concentration of metal cations (Fe^{3+} and M^{2+}) was 1 M. Scale bar in TEM image (inset of (a)) is 100 nm.

hydrothermal process. Series of experiments were carried out to prepare ferrite hollow spheres with gold NP cores to further demonstrate the generality of this method. The process was the same with that used to prepare ferrite hollow spheres with silver NP cores: using colloidal Au@C core–shell spheres instead of Ag@C as templates for adsorption of metal cations (Fe^{3+} and M^{2+}) and followed by a calcination process. The final products were successfully obtained and characterized by TEM, SEM and XRD. As shown in Fig. 12, the size of zinc ferrite hollow spheres with gold cores was in the range of 160–180 nm and the shell was very thin (about 20 nm) when total concentration of metal cations was 1 M. The XRD pattern shown in Fig. 12b can be perfectly indexed as fcc phase zinc ferrite (JCPDS no. 22-1012). Additionally, five diffraction peaks are observed at $2\theta = 38.2^\circ$, 44.3°, 64.5°, 77.6° and 81.6°, corresponding to the (111), (200), (220), (311) and (222) reflections of fcc structured metal Au (PDF 04-0784), respectively.

4. Conclusions

In summary, MFe_2O_4 (M = Ni, Co, Mg, Zn) hollow spheres with a noble metal NP core are successfully prepared by using colloidal metal@C core–shell spheres as templates with no need of surface modification. The shell thickness and magnetic properties of the ferrite hollow spheres could be controlled by varying the synthetic parameters. The resulted composites possessed good antibacterial activities and superparamagnetic behaviors at room temperature with which the composites could be easily and rapidly separated from the solution. We believe that this is a general, simple and cheap approach for obtaining various jingle-bell-shaped metal ferrite hollow spheres functionalized with metal NP cores especially noble metal particles. The preparation of metal@C microspheres used water as environmentally benign solvent and glucose as reducing reagent, and no toxic reagents were used. Moreover, during the calcination procedure, the carbon shell of the templates transforms into CO_2, which is environmentally circular gas. This simple fabrication strategy may open an avenue for the low cost and facile preparation of multifunctional jingle-bell-shaped composites. We also believe that this type of materials would be of importance in the growing field of advanced nanomaterials and nanotechnology.

Supplementary data

Supplementary data provides details about the synthesis of Au@C core–shell colloids, TEM images of Au@C core–shell colloids and the component of culture medium LactoseBroth (LB).

Acknowledgments

This work was supported by the National Natural Science Foundation of China (Nos. 20701005/20701006); the Science and Technology Development Project Foundation of Jilin Province (No. 20060420); the Postdoctoral station Foundation of Ministry of Education (No. 20060200002); the Testing Foundation of Northeast Normal University; the Program for Changjiang Scholars and Innovative Research Team in University.

Appendix A. Supplementary materials

Supplementary data associated with this article can be found in the online version at doi:10.1016/j.jssc.2008.05.021.

References

[1] H. Zhu, M.J. McShane, J. Am. Chem. Soc. 127 (2005) 13446.
[2] M.S. Fleming, T.K. Mandal, D.R. Walt, Chem. Mater. 13 (2001) 2210.
[3] L. Wang, T. Sasaki, Y. Ebina, K. Kurashima, M. Watanabe, Chem. Mater. 14 (2002) 4827.
[4] E.V. Parthasarathy, C.R. Martin, J. Appl. Polym. Sci. 62 (1996) 875.
[5] M.C. Daniel, D. Astruc, Chem. Rev. 104 (2005) 293.
[6] C.D. Grant, A.M. Schwartzberg, T.J. Norman Jr., J.Z. Zhang, J. Am. Chem. Soc. 125 (2003) 551.
[7] J.W. Stone, P.N. Sisco, E.C. Goldsmith, S.C. Baxter, C.J. Murphy, Nano Lett. 7 (2007) 116.
[8] N.L. Rosi, C.A. Mirkin, Chem. Rev. 105 (2005) 1547.
[9] F. Caruso, Adv. Mater. 13 (2001) 11.
[10] P. Schuetz, F. Caruso, Chem. Mater. 16 (2004) 3066.
[11] A. Dowson, P.V. Kamat, J. Phys. Chem. B 105 (2001) 960.
[12] C. Pacholski, A. Kornowski, H. Weller, Angew. Chem. Int. Ed. 43 (2004) 4774.
[13] M. Jokob, H. Levanon, Nano Lett. 3 (2003) 353.
[14] K.T. Lee, Y.S. Jung, S.M. Oh, J. Am. Chem. Soc. 125 (2003) 5652.
[15] S. Gu, T. Kondo, E. Mine, D. Nagao, Y. Kobayashi, M. Konno, J. Colloid Interface Sci. 279 (2004) 281.
[16] K. Zhang, X. Zhang, H. Chen, X. Chen, L. Zheng, J. Zhang, B. Yang, Langmuir 20 (2004) 11312.
[17] K. Kamata, Y. Lu, Y. Xia, J. Am. Chem. Soc. 125 (2003) 2384.
[18] F. Liang, L. Guo, Q.P. Zhong, Appl. Phys. Lett. 89 (2006) 103105.
[19] X.M. Sun, Y.D. Li, Angew. Chem. Int. Ed. 43 (2004) 597.
[20] X.M. Sun, Y.D. Li, Langmuir 21 (2005) 6019.
[21] X.M. Sun, Y.D. Li, Angew. Chem. Int. Ed. 43 (2004) 3827.
[22] X.M. Sun, J.F. Liu, Y.D. Li, Chem. Eur. J. 12 (2006) 2039.
[23] D.S. Koktysh, X.R. Liang, B.G. Yun, I. Pastoriza-Santos, R.L. Matts, M. Giersig, C. Serra-Rodriguez, L.M. Liz-Marzan, N.A. Kotov, Adv. Funct. Mater. 12 (2002) 255.
[24] T. Torimoto, J.P. Reyes, K. Iwasaki, B. Pal, T. Shibayama, K. Sugawara, H. Takahashi, B. Ohtani, J. Am. Chem. Soc. 125 (2003) 316.
[25] K. Iwasaki, T. Torimoto, T. Shibayama, H. Takahashi, B. Ohtani, J. Phys. Chem. B 108 (2004) 11946.
[26] Y. Kobayashi, V. Salgueirino-Maceira, L.M. Liz-Marzan, Chem. Mater. 13 (2001) 1630.
[27] C. Petit, P. Lixon, M.P. Pileni, J. Phys. Chem. 97 (1993) 12974.
[28] H. Ohde, F. Hunt, C.M. Wai, Chem. Mater. 13 (2001) 4130.
[29] Y. Shon, E. Cutler, Langmuir 20 (2004) 6626.
[30] Y.Q. Chu, Z.W. Fu, Q.Z. Qin, Electrochim. Acta 49 (2004) 4915.
[31] L. Fu, X. Liu, Y. Zhang, V.P. Dravid, C.A. Mirkin, Nano Lett. 3 (2003) 757.
[32] T. Bala, C.R. Sankar, M. Baidakova, V. Osipov, T. Enoki, P.A. Joy, B.L.V. Prasad, M. Sastry, Langmuir 21 (2005) 10638.
[33] C.J. Powell, Appl. Surf. Sci. 89 (1995) 141.
[34] E. Mathiowitz, J.S. Jacob, Y.S. Jong, G.P. Carino, D.E. Chickering, P. Chaturvedi, C.A. Santos, K. Vijayaraghavan, S. Montgomery, M. Bassett, C. Morrell, Nature 386 (1997) 410.
[35] H.T. Schmidt, A.E. Ostafin, Adv. Mater. 14 (2002) 532.
[36] M.E. Olson, J.B. Wright, K. Lam, R.E. Burrell, Eur. J. Surg. 166 (2000) 486.
[37] C. Aymonier, U. Schlotterbeck, L. Antonietti, P. Zacharias, R. Thomann, J.C. Tiller, S. Mecking, Chem. Commun. (2002) 3018.
[38] A. Melaiye, Z. Sun, K. Hindi, A. Milsted, D. Ely, D.H. Reneker, C.A. Tessier, W.J. Youngs, J. Am. Chem. Soc. 127 (2005) 2285.
[39] R.W. Sun, R. Chen, N.P. Chung, C.M. Ho, C.L. Lin, C.M. Che, Chem. Commun. (2005) 5059.
[40] C.N. Lok, C.M. Ho, R. Chen, Q.Y. He, W.Y. Yu, H.Z. Sun, P.K.H. Tam, J.F. Chiu, C.M. Che, Biol. Inorg. Chem. 12 (2007) 527.